#### Early Tetrapodomorph Biogeography: Controlling for Fossil Record **Bias in Macroevolutionary Analyses** Jacob D. Gardner<sup>a,1</sup>, Kevin Surya<sup>b,1</sup>, and Chris L. Organ<sup>a</sup>\* <sup>a</sup> Department of Earth Sciences, Montana State University, Bozeman, MT 59717, USA <sup>b</sup> Honors College, Montana State University, Bozeman, MT 59717, USA \* Corresponding author at: Department of Earth Sciences, Montana State University, Bozeman, MT 59717, USA. E-mail address: organ@montana.edu (C. L. Organ) <sup>1</sup> Contributed equally to this work

#### 

### 47 ABSTRACT

The fossil record provides direct empirical data for understanding macroevolutionary patterns and processes. Inherent biases in the fossil record are well known to confound analyses of this data. Sampling bias proxies have been used as covariates in regression models to test for such biases. Proxies, such as formation count, are associated with paleobiodiversity, but are insufficient for explaining species dispersal owing to a lack of geographic context. Here, we develop a sampling bias proxy that incorporates geographic information and test it with a case study on early tetrapodomorph biogeography. We use recently-developed Bayesian phylogeographic models and a new supertree of early tetrapodomorphs to estimate dispersal rates and ancestral habitat locations. We find strong evidence that geographic sampling bias explains supposed radiations in dispersal rate (potential adaptive radiations). Our study highlights the necessity of accounting for geographic sampling bias in macroevolutionary and phylogenetic analyses and provides an approach to test for its effect.

*Keywords: sampling bias, fossil record, biogeography, phylogenetics, macroevolution, tetrapod water-land transition* 

#### 2

#### 70 1. Introduction

71 Our understanding of macroevolutionary patterns and processes are fundamentally based 72 on fossils. The most direct evidence for taxonomic origination and extinction rates come from the 73 rock record, as do evidence for novelty and climate change unseen in data sets gleaned from extant 74 sources. There are no perfect data sets in science; there are inherent limitations and biases in the 75 rock record that must be addressed when we form and test paleobiological hypotheses. For instance, observed stratigraphic ranges of fossils can mislead inferences about diversification and extinction 76 rates (Raup and Boyajian, 1988; Signor and Lipps, 1982). Observed species diversity is also known 77 78 to increase with time due to the preferential preservation and recovery of fossils in younger 79 geological strata—referred to as "the Pull of the Recent" (Jablonski et al., 2003). Large and long-80 surviving clades with high rates of early diversification tend to result in an illusionary rate slow-81 down as diversification rates revert back to a mean value-referred to as "the Push of the Past" (Budd and Mann, 2018). Paleobiologists test and account for these biases when analyzing 82 83 diversification and extinction at local and global scales (Alroy et al., 2001; Benson et al., 2010; 84 Benson and Butler, 2011; Benson and Upchurch, 2013; Benton et al., 2013; Foote, 2003; Jablonski 85 et al., 2003; Koch, 1978; Lloyd, 2012; Sakamoto et al., 2016a, 2016b). These bias-detection and 86 correction techniques include fossil occurrence subsampling (Alroy et al., 2001; Jablonski et al., 2003; Lloyd, 2012); correcting origination, extinction, and sampling rates using evolutionary 87 88 predictive models (Foote, 2003); the use of residuals from diversity-sampling models (Benson et 89 al., 2010; Benson and Upchurch, 2013; Sakamoto et al., 2016b); and the incorporation of sampling bias proxies as covariates in regression models (Benson et al., 2010; Benson and Butler, 2011; 90 91 Benton et al., 2013; Sakamoto et al., 2016a). Benton et al. (2013), studying sampling bias proxies, 92 demonstrated that diversity through time closely tracks formation count (Benton et al., 2013).

3

93 However, case studies in England and Wales suggest that proxies for terrestrial sedimentary rock 94 volume (such as formation count) do not accurately explain paleobiodiversity, particularly if the fossil record is patchy (Dunhill et al., 2014a, 2014b, 2013). Marine outcrop area and 95 paleoecological-associated facies changes are, however, associated with shifts in paleobiodiversity 96 97 (Dunhill et al., 2014b, 2013). Moreover, Benton et al. (2013) argue that the direction of causality 98 between paleobiodiversity and formation count is unclear; there may be a common cause to explain 99 their covariation, such as sea level (Benton et al., 2013). Nonetheless, formation count is a widelyused sampling bias proxy in phylogenetic analyses of macroevolution (O'Donovan et al., 2018; 100 101 Sakamoto et al., 2016a, 2016b; Tennant et al., 2016a, 2016b). The advent of computational 102 modeling approaches, particularly phylogenetic comparative methods, has made it easier to 103 include proxies, like formation count, into models. Additional sampling bias proxies used in these 104 studies include occurrence count, valid taxon count, and specimen completeness and preservation 105 scores. Absent from these proxies is geographic context, which could confound many types of 106 macroevolutionary analyses.

107 Despite advancements made in understanding the origin and evolution of early 108 tetrapodomorphs, biogeographical studies are hindered by the incompleteness of the early 109 tetrapodomorph fossil record. For example, "Romer's Gap" represents a lack of tetrapodomorph 110 fossils from the end-Devonian to mid-Mississippian, a period crucial for understanding early 111 tetrapodomorph diversification. Recent collection efforts recovered tetrapodomorph specimens 112 from "Romer's Gap", suggesting that a collection and preservation bias explains this gap (Clack 113 et al., 2017; Marshall et al., 2019). In addition, a trackway site in Poland demonstrates the existence 114 of digit-bearing tetrapodomorphs 10 million years before the earliest elpistostegalian body fossil, 115 showcasing the limitation of body fossils to reveal evolutionary history (Niedźwiedzki et al., 2010).

4

A recent study by Long et al. (2018) leveraged phylogenetic reconstruction of early tetrapodomorphs to frame hypotheses about the origin of major clades, as well as their dispersal patterns, including the hypothesis that stem-tetrapodomorphs dispersed from Eastern Gondwana to Euramerica. However, this study did not use phylogenetic comparative methods to estimate ancestral geographic locations or to model dispersal patterns.

121 Here, we present a phylogeographic analysis of early tetrapodomorphs. Our goals are: 1) 122 to construct a phylogenetic supertree of early tetrapodomorphs that synthesizes previous 123 phylogenetic reconstructions; 2) to estimate the paleogeographic locations of major early 124 tetrapodomorph clades using recently-developed phylogeographic models that account for the 125 curvature of the Earth; and 3) to test for the influence of geographic sampling bias on dispersal 126 rates. Our results indicate that geographic sampling bias substantially confounds analyses of 127 dispersal and paleogeography. We conclude with a discussion about the necessity of controlling for fossil record biases in macroevolutionary analyses. 128

- 129 2. Materials and Methods
- 130 2.1. Nomenclature

131 Tetrapoda has been informally defined historically to include all terrestrial vertebrates with 132 limbs and digits (Laurin, 1998). Gauthier et al. (1989) first articulated a phylogenetic definition of 133 Tetrapoda as the clade including the last common ancestor of amniotes and lissamphibians. This 134 definition excludes stem-tetrapodomorphs, like Acanthostega and Ichthyostega. Stegocephalia 135 was coined by E.D. Cope in 1868 (Cope, 1868), but was more recently used to describe fossil taxa 136 more closely related to tetrapods than other sarcopterygians. A recent cladistic redefinition of 137 Stegocephalia includes all vertebrates more closely related to temnospondyls than *Panderichthys* 138 (Laurin, 1998). Here, we use the definitions of Laurin (1998) for a monophyletic Stegocephalia

and of Gauthier et al. (1989) for Tetrapoda, which refers specifically to the crown group. We use Tetrapodomorpha to refer to all taxa closer to the tetrapod crown-group than the lungfish crowngroup (Ahlberg, 1998). We additionally use Elpistostegalia (= Panderichthyida) to refer to the common ancestor of all stegocephalians and *Panderichthys* as well as Eotetrapodiformes to refer to the common ancestor of all tristichopterids, elpistostegalians, and tetrapods (Coates and Friedman, 2010).

145 *2.2. Supertree* 

We inferred a supertree of 69 early tetrapodomorph taxa from five edited, published 146 147 morphological data matrices, focusing on tetrapodomorphs whose previously inferred 148 phylogenetic position bracket the water-land transition (Clack et al., 2017; Friedman et al., 2007; 149 Pardo et al., 2017; Swartz, 2012; Zhu et al., 2017). Since downstream analyses might be sensitive 150 to unequal sample sizes between taxa pre- and post-water-land transition, we did not include several crownward stem-tetrapodomorphs from the original matrices (see Supplementary 151 152 Material). For each matrix, we generated a posterior distribution of phylogenetic trees using 153 MrBayes 3.2.6 (Ronquist et al., 2012b). In each case, we ran two Markov chain Monte Carlo 154 (MCMC) replicates for 20,000,000 generations with 25% burn-in, each with four chains and a 155 sampling frequency of 1,000. We used one partition, except for Clack et al.'s (2017) matrix, which 156 was explicitly divided into cranial and postcranial characters. To time-calibrate the trees, we 157 constrained the root ages and employed a tip-dating approach (Ronquist et al., 2012a). Tip dates 158 (last occurrence) were acquired from the Paleobiology Database (PBDB; https://paleobiodb.org/) and the literature (see Supplementary Table 2). Root calibrations (minimum and soft maximum 159 160 age estimates) were collected from the PBDB and Benton et al. (2015). We also used the fossilized 161 birth-death model as the branch length prior (Didier et al., 2017, 2012; Didier and Laurin, 2018;

6

Gavryushkina et al., 2014; Heath et al., 2014; Stadler, 2010; Zhang et al., 2016). All pairs of
MCMC replicates converged as demonstrated by low average standard deviation of split
frequencies (<0.005; Lakner et al., 2008; see Supplementary Table 3).</li>

165 Next, we used the five maximum clade credibility trees (source trees; Supplementary Fig. 166 1-10) to compute a distance supermatrix using SDM 2.1 (Criscuolo et al., 2006). We then inferred 167 an unweighted neighbor-joining tree (UNJ by Gascuel, 1997) from the distance supermatrix using 168 PhyD\* 1.1 (Criscuolo and Gascuel, 2008). The UNJ\* algorithm is preferable for matrices based 169 on morphological characters. Unlike most supertree methods, the SDM-PhyD\* combination 170 produces a supertree with branch lengths. We rooted the supertree using phytools 0.6.60 (Revell, 171 2012) by adding an arbitrary branch length of 0.00001 to break the trichotomy at the basal-most 172 node in R 3.5.2 (R Core Team, 2018), designating the dipnomorph *Glyptolepis* as the outgroup.

We qualitatively compared the supertree topology with the published source trees and Marjanović and Laurin's (2019) Paleozoic limbed vertebrate topologies. We also calculated normalized Robinson-Foulds (nRF) distances (Robinson and Foulds, 1981) using phangorn 2.4.0 (Schliep, 2011) in R to assess the congruency of topologies. In each comparison, polytomies in the supertree or the source tree were resolved in all possible ways using phytools. We then calculated all nRF distances and took an average (see Supplementary Table 4). The supplementary materials include a more detailed description of this approach.

180 *2.3. Phylogeography* 

We obtained paleocoordinate data (paleolatitude and paleolongitude) for 63 early tetrapodomorphs from the PBDB using the GPlates software setting (<u>https://gws.gplates.org/</u>). By default, GPlates estimates paleocoordinates from the midpoint of each taxon's age range. For 16 taxa that did not have direct paleocoordinate data in the PBDB, we searched for the geological

185 formations and geographic regions within the time range from which they are known and averaged 186 the paleolocations across each valid taxonomic occurrence in the PBDB. If the paleolocation of 187 the formation was not listed in the PBDB, we used published geographic locations of the 188 formations. This level of precision is adequate for world-wide phylogeographic analyses, such as 189 conducted here. Present-day coordinates for these geographic locations were obtained from 190 Google Earth and matched with PBDB entries that date within each taxon's age range (see 191 Supplementary Table 5). Four additional taxa, Kenichthys, Koilops, Ossirarus, and Tungsenia, had 192 occurrences in the PBDB but the GPlates software could not estimate their paleocoordinates. For 193 Koilops and Ossirarus, we used all tetrapodomorph occurrences from the Ballagan Formation of 194 Scotland, UK—a formation in which these two taxa are found (Clack et al., 2017). For Kenichthys 195 and *Tungsenia*, we calculated paleocoordinate data from the GPlates website directly using the 196 present-day coordinates from the PBDB (https://gws.gplates.org/#recon-p). This approach did not work for the 16 previously mentioned taxa (see Supplementary Table 5). We therefore obtained 197 198 paleocoordinate data from nearby entries in the PBDB. We excluded the following taxa from our 199 analyses due to the lack of data and comparable entries in the PBDB: Jarvikina, Koharalepis, 200 Spodichthys, and Tinirau. We excluded the outgroup taxon, Glyptolepis, in our analysis to focus 201 on the dispersal trends within early Tetrapodomorpha. We also excluded Eusthenodon and 202 Strepsodus because their high estimated dispersal rates-being reported from multiple 203 continents—masked other rate variation throughout the phylogeny and inhibited our downstream 204 analyses from converging on a stable likelihood. We do, however, discuss their geographic 205 implications in Section 4.

A model that incorporates phylogeny is crucial for paleobiogeographic reconstruction because it accounts for both species relationships and the amount of evolutionary divergence

8

208 (branch lengths). Using continuous paleocoordinate data, rather than discretely-coded regions, 209 allows dispersal trends to be estimated at finer resolutions. Discretely-coded geographic regions 210 also limit ancestral states to the same regions inhabited by descendant species. However, standard 211 phylogenetic comparative methods for continuous data assume a flat Earth because they do not 212 account for spherically structured coordinates (i.e., the proximity of  $-179^{\circ}$  and  $179^{\circ}$  longitudes). 213 Recently-developed phylogenetic comparative methods for modeling continuous paleocoordinate 214 data, implemented as the 'geo' model in the program BayesTraits V3, overcome this hurdle by 215 "evolving" continuous coordinate data on the surface of a globe (O'Donovan et al., 2018). The 216 model is implemented with a Bayesian reversible jump MCMC algorithm to estimate rates of 217 geographic dispersal and ancestral paleolocations simultaneously. To account for the spheroid 218 shape of the globe, the 'geo' model converts latitude and longitude data into three-dimensional 219 coordinates while prohibiting moves that penetrate the inside of the globe. Ancestral states, which 220 are converted back to standard latitude and longitude, are estimated for each node of the phylogeny. 221 The method includes a variable rates model to estimate variation in dispersal rate (Venditti et al., 222 2011). The 'geo' model makes no assumptions about the location of geographic barriers or 223 coastlines, but a study on dinosaur biogeography found 99.2% of mean ancestral state 224 reconstructions to be located within the bounds of landmasses specific to the time at which they 225 occurred (O'Donovan et al., 2018). We ran three replicate independent analyses using the Bayesian 226 phylogenetic 'geo' model for 100 million iterations each with a 25% burn-in and sampling every 227 1,000 iterations. We estimated log marginal likelihoods using the Stepping Stone algorithm with 228 250 stones sampling every 1,000 iterations (Xie et al., 2011). We used Bayes factors (BF) to test 229 whether a variable rates model explained the data better than a uniform rates model. Bayes factors 230 greater than two are considered good evidence in support of the model with the greater log

marginal likelihood. We compared estimated rate scalars and ancestral states among the three
independent variable rates analyses to check for consistency in our results. Rates of dispersal were
estimated for each branch by dividing the average rate scalars by the original branch lengths
(scaled by time). We assessed the MCMC convergence of all analyses using Tracer 1.7 (Rambaut
et al., 2018).

236 To test for the effect of sampling bias on dispersal rates, we developed a sampling bias 237 proxy that incorporates geographic context: regional-level formation count. Formation counts are 238 meant to capture multiple biases: uneven global rock exposure, uneven fossil collection and 239 database efforts, and global variation in sediment deposition in environments conducive to 240 preservation. Stage-level (stage-specific) formation count represents the mean number of 241 formations, or distinct rock units, globally known to produce relevant fossils along each terminal 242 branch of a phylogeny. Following the protocol of Sakamoto et al. (2016) and O'Donovan et al. 243 (2018), stage-level formation counts are calculated by taking the average number of formations 244 known from each geological age across the globe that encompass the time period between the 245 taxon's tip date and its preceding node. These average stage-level formation counts are weighted 246 by the proportion that each terminal branch length covers each geological age. For example, if a 247 terminal branch covers two geological ages (e.g., Frasnian and Famennian) at 30% and 70%, 248 respectively, then the stage-level formation counts from each geological age are weighted by those 249 proportions and then divided by the number of geological ages covered:

250

251 Stage – Level FormationCount = 
$$\frac{\text{FrasnianCount} \times 0.3 + \text{FamennianCount} \times 0.7}{2}$$

252

253

Stage-level formation count is not informed by geography; it is a global metric. It is

254 therefore an inadequate proxy if bias has a strong geographic component (e.g., if the majority 255 of formations recorded are from a specific region or if few formations are exposed within a region). 256 The number of fossil-bearing geological formations, accounting for geographic distribution, is 257 expected to be an important confounding bias in the fossil record. We developed a proxy that 258 includes geographic sampling bias. Our approach breaks down stage-level formation count by 259 geographic region. To account for the arrangement of the continents during the Devonian, Carboniferous, and Permian, we recognized five major regions: Northern Euramerica (including 260 Northeastern Eurasia and Central Asia), Southern Euramerica (North America, Greenland, and 261 262 Western Europe), Western Gondwana (South America and Africa), Eastern Gondwana (Antarctica, 263 Australia, and Southern Asia), and East Asia (e.g., China). For each branch in the phylogeny, we 264 used the average ancestral state and taxon paleolocation estimates to determine if the branch 265 crossed multiple geographic regions. The number of formations within this time window are totaled for every region covered by the branch and then divided by the number of regions covered. For example, if ancestral state estimates at node 1 and 2 are located in Eastern Gondwana and 267 268 Southern Euramerica, respectively, then the number of formations recorded in Eastern Gondwana, 269 Southern Euramerica, and the regions in between (i.e., Western Gondwana or Northern Euramerica 270 + East Asia) are counted for that geological age; this total is then divided by the number of 271 geographic regions covered by the entire branch (three for the Western Gondwana route and four 272 for the Northern Euramerica + East Asia route). If the dispersal path between two consecutive 273 ancestral states does not cross any of the five regions, then the number of formations in the 274 inhabited region is counted alone. Figure 1 illustrates an example of how this proxy is measured. 275 This results in the average number of formations present along the dispersal path (at geographic 276 region scale) for each branch in the phylogeny. As with stage-level formation counts, the regional-

11

277 level formation counts are weighted by the proportion that the branch length covers each geological age. We hypothesize that dispersal rate will inversely correlate with regional-level formation count 278 279 because we expect that the lack of formations in intermediate regions will lead to inflated dispersal 280 rates. The 'geo' model will increase the dispersal rate along a branch to account for the geographic 281 variation observed when there is a lack of intermediate geographic fossil occurrences. This hypothesis can be falsified if high dispersal rates are associated with larger average numbers of 282 283 formations along dispersal paths. Benton et al. (2013) provide a global sample of tetrapod-bearing 284 rock formations known for each geological age from the Middle Devonian through the Triassic. 285 We supplemented these lists with stratigraphic units known to produce sarcopterygian fossils entered in the PBDB (collected on December 10<sup>th</sup>, 2018). 286

Period	Epoch	Age	End Time (Ma)	Northern Euramerica	Southern Euramerica	Western Gondwana	Eastern Gondwana	East Asia	Total
Permian	Cisuralian	Kungurian	272.95	10	44	11	0	0	65
Permian	Cisuralian	Artinskian	283.5	2	39	9	0	0	50
Permian	Cisuralian	Sakmarian	290.1	2	44	4	0	0	50
Permian	Cisuralian	Asselian	295	2	47	3	0	0	52
Pennsylvanian	Late	Gzhelian	298.9	1	42	0	0	0	43
Pennsylvanian	Late	Kasimovian	303.7	0	33	0	0	0	33
Pennsylvanian	Middle	Moscovian	307	0	16	0	0	0	16
Pennsylvanian	Early	Bashkirian	315.2	0	28	0	0	0	28
Mississippian	Late	Serpukhovian	323.2	0	16	0	0	0	16
Mississippian	Middle	Viséan	330.9	0	14	0	1	0	15
Mississippian	Early	Tournaisian	346.7	0	7	0	1	0	8
Devonian	Late	Famennian	358.9	1	9	1	5	1	17
Devonian	Late	Frasnian	372.2	1	11	0	3	2	17
Devonian	Middle	Givetian	382.7	1	8	1	4	1	15
Devonian	Middle	Eifelian	387.7	1	8	0	5	2	16
Devonian	Early	Emsian	393.3	2	5	0	7	3	17
Devonian	Early	Pragian	407.6	1	6	0	4	2	13
Devonian	Early	Lochkovian	410.8	1	3	0	3	1	8
Silurian	Přídolí	Přídolí	419.2	0	0	0	0	1	1
Silurian	Ludlow	Ludfordian	423	0	0	0	0	2	2
Silurian 87							2		

12

288

289 To test for the effect of regional-level formation count bias on dispersal rate, we conducted a non-parametric two-sample, upper-tailed Mann-Whitney U-test using the base package 'stats' in 290 291 R (R Core Team, 2018). This approach ranks all branches of the phylogeny by their regional-level 292 formation count and tests if the branches with lower dispersal rates rank higher on average than 293 branches with higher rates. We define "high" vs "low" dispersal rates based on whether or not they 294 are two standard deviations greater than the average rate across the tree. Due to the vast difference in sample size between the two groups ("high rates": n = 9, "low rates": n = 111), we bootstrapped 295 296 the regional-level formation counts from each group with 100,000 replicates. From this bootstrap analysis, we obtained a 95% confidence interval for the summed ranks of the branches with low 297 298 dispersal rates (n = 100,000 U-statistic values). The expected U-statistic is 499.5 given the null 299 hypothesis that only 50% of the regional-level formation counts along branches with low rates rank higher than the formation counts with high rates (half of all possible combinations =  $\frac{9 \times 111}{2}$ ). 300 A 95% confidence interval of bootstrapped U-statistics that does not include the null expected U-301 302 statistic is considered good evidence for higher mean dispersal rates along branches with lower regional-level formation counts. The full dataset and code for the phylogeographic analyses can 304 be requested by email to the corresponding author.

Estimated ancestral states do not identify specific dispersal routes, so we conducted sensitivity analyses to test if the dispersal route chosen for counting formations influenced our results. We conceived of three scenarios for dispersal routes between Eastern Gondwana and Southern Euramerica or vice versa: 1) a dispersal route through Western Gondwana; 2) a route through Northern Euramerica and East Asia; and 3) a direct route between Eastern Gondwana and Southern Euramerica. For the first scenario, we averaged the number of formations found in

13

Eastern and Western Gondwana and Southern Euramerica for a given time period. The second scenario is similar to the first but included formation counts from Northern Euramerica and East Asia in place of Western Gondwana. The third scenario only averaged formation counts from Eastern Gondwana and Southern Euramerica.

315 **3. Results** 

316 *3.1. Supertree* 

317 Topological differences resulted among our supertree, the published source trees, and 318 Marjanović and Laurin's (2019) tree (Figure 2). In our tree, a polyphyletic "Megalichthyiformes" 319 is the basal-most tetrapodomorph group instead of Rhizodontida (Swartz, 2012; Zhu et al., 2017). Canowindrids and rhizodontids formed an unexpected sister clade to Eotetrapodiformes. Clack et 321 al.'s (2017) five Tournaisian tetrapod taxa cluster together. Colosteidae is rootward of 322 Crassigyrinus. Caerorhachis is next to Baphetidae. Baphetidae moved crownward compared to 323 previous topologies (likely because of a small character sample size [Marjanović and Laurin, 324 2019]). Two crownward nodes are unresolved (polytomous). We retained Tungsenia and 325 Kenichthys as the oldest and second oldest tetrapodomorphs. Tristichopteridae, Elpistostegalia, 326 Stegocephalia, Aïstopoda, Whatcheeriidae, Colosteidae, Anthracosauria, Dendrerpetidae, and 327 Baphetidae remain monophyletic. Aïstopoda (Lethiscus and Coloraderpeton) fell rootward to Tetrapoda as reported in Pardo et al. (2017; 2018). The average nRF distances quantify differences 328 329 in topology (see Supplementary Table 4). On average, there are 39.7% different or missing bipartitions in the source trees compared to the supertree.

331 *3.2. Phylogeography* 

We found overwhelming support for a variable rates model of geographic dispersal in early tetrapodomorphs (BF = 632.3; Figure 3). The estimated rates across the three replicate runs are

334 consistent (out of 122 branches, only three had a median rate scalar with an absolute value 335 difference among the three runs greater than 3). All rate shifts that were two standard deviations 336 greater than the average dispersal rate were reconstructed dispersal events moving from East Asia 337 to Southern Euramerica, from Eastern Gondwana to Southern Euramerica, or Southern Euramerica 338 to Eastern Gondwana. The fastest estimated dispersal rate occurs along the branch leading to 339 Eotetrapodiformes, moving from Eastern Gondwana to Southern Euramerica (14.34x the average 340 rate). As Long et al. (2018) suggest, we find evidence for an East Asian origin for Tetrapodomorpha but with moderate uncertainty (average estimate  $\pm$  standard deviation of posterior distribution; 341 longitude<sub>avg</sub> =  $81.5^{\circ} \pm 10.1^{\circ}$ , latitude<sub>avg</sub> =  $-6.4^{\circ} \pm 8.5^{\circ}$ ). We also reconstruct an origin for 342 "Megalichthyiformes" that borderlines East Asia and Eastern Gondwana (longitude<sub>avg</sub> =  $107.2^{\circ} \pm$ 343 14.1°, latitude<sub>avg</sub> =  $-22.6^{\circ} \pm 8.7^{\circ}$ ), along with an Eastern Gondwana origin for the clade uniting 344 345 "Canowindridae" and Rhizodontida (longitude<sub>avg</sub> =  $137.1^{\circ} \pm 8.2^{\circ}$ , latitude<sub>avg</sub> =  $-32.0^{\circ} \pm 4.7^{\circ}$ ). We recover a Southern Euramerican origin for Eotetrapodiformes, consistent with previous studies 346 (longitude<sub>avg</sub> =  $-12.5^{\circ} \pm 7.0^{\circ}$ , latitude<sub>avg</sub> =  $-19.4^{\circ} \pm 6.4^{\circ}$ ). A Southern Euramerican origin was also 347 found for Tristichopteridae (longitude<sub>avg</sub> =  $-12.7^{\circ} \pm 6.9^{\circ}$ , latitude<sub>avg</sub> =  $-19.7^{\circ} \pm 6.3^{\circ}$ ) and 348 Elpistostegalia (longitude<sub>avg</sub> =  $-12.3^{\circ} \pm 5.5^{\circ}$ , latitude<sub>avg</sub> =  $-13.5^{\circ} \pm 5.3^{\circ}$ ). As expected in a 349 phylogenetic comparative analysis, uncertainty in estimated node states increases toward the root. 351 However, despite the level of uncertainty within a single run, only three nodes have mean ancestral state values that are greater than an absolute value of 5° among the replicate three runs. 352

We find good evidence that geographic sampling bias influences dispersal rate estimates, regardless of the route used (95% CI: Western Gondwana route U = [800, 928]; Northern Euramerica + East Asia route U = [832, 946]; direct route U = [729, 889]; no scenario includes the null U = 499.5; Figure 4 and Supplementary Figures 12-13). A U-statistic considerably higher than

357 499.5 suggests that branches with high dispersal rates have lower regional-level formation counts, 358 on average, than branches with low rates. One can also interpret the null U-statistic of 499.5 as a 359 50% probability that a random branch with a low dispersal rate will rank higher in its regional-360 level formation count than a random branch with a high dispersal rate. With bootstrapping, we are 361 95% confident that the probability of a random branch with a low dispersal rate having a higher regional-level formation count than a random branch with a high rate is 72.97-88.99% for the 362 more conservative 'direct route' scenario. Under the more liberal 'Northern Euramerica + East 363 Asia route' scenario, the probabilities are 83.28–94.69%. In sum, branches with high dispersal 364 365 rates (two standard deviations greater than average) have a smaller number of recorded formations, 366 on average, along their reconstructed dispersal path.

Our results cannot be explained by a fossil record that is more complete through time (Pull of 367 368 the Recent). A regression model relating regional-level formation count to the minimum age of each branch shows only a weak relationship (slope = -0.044,  $r^2 = 0.1$ , P < 0.001). However, total 369 370 global (stage-level) formation count (which does not account for geographic variation) does show potential bias from Pull of the Recent (slope = -0.3,  $r^2 = 0.71$ , P < 0.0001). If dispersal rates are 371 372 biased by the increase in number of formations globally, we would also expect to see elevated 373 dispersal rates decrease toward the tips, but a regression model relating stretched branch lengths with time is not supported (slope = -0.025,  $r^2 = 0.006$ , P = 0.41). 374

#### 375 **4. Discussion**

We expected to infer high dispersal rates for closely related taxa that are distributed across the globe. Our results, unadjusted for geographic bias in the fossil record, confirm this notion. However, we also find a compelling statistical association between high dispersal rates and a low number of formations along dispersal paths—a patchy fossil record is driving inferences of high

380 dispersal rates. Although we did not test for a correlation between dispersal rate and previously 381 used proxies, such as valid taxon count and stage-level formation count, these proxies do not offer 382 clear predictions for explaining dispersal rate variation. High dispersal rate variation is inferred 383 when closely related taxa are geographically separate. For example, valid taxon count cannot 384 explain geographic rate variation because spatial information is lacking in this bias proxy and 385 because sister taxa are likely to have similar counts (these data are phylogenetically structured). Stage-level formation counts will also not explain dispersal rate variation, particularly if high rate 386 variation exists within the same geological age. Assuming geological formations are evenly 387 388 exposed and sampled worldwide, low stage-level formation counts should yield geographically 389 variable fossil species and, therefore, drive high dispersal rate variation. However, formations are 390 not evenly exposed or recorded in geological/paleontological databases, including the PBDB. Our 391 formation count table demonstrates this bias (Table 1). Without geographic context, stage-level formation count cannot distinguish between global and local regions. For example, the geological 392 393 ages that have the highest recorded number of formations are restricted to Southern Euramerica 394 where the majority of eotetrapodiform taxa have been discovered. The association between high 395 formation counts in specific regions and high paleobiodiversity in those regions is likely not a 396 coincidence and has a clear impact on how we interpret dispersal history. The earliest 397 tetrapodomorphs are known from China and Australia at geological ages where relatively few 398 formations are recorded outside of East Asia and Eastern Gondwana. The basal-most ancestral 399 state estimates reconstruct paleolocations in East Asia (not surprisingly). This inference (hypothesis) is predicated on the lack of geological formations recorded outside of East Asia during 400 401 this time period. In addition, the majority of more crownward taxa and their reconstructed ancestral 402 states are located in North America and Europe at geological ages in which relatively fewer

17

403 formations are known elsewhere. This bias may heavily influence any conclusions made on the 404 location and habitat of the tetrapod water-land transition. Recently discovered taxa could help 405 mitigate this problem by increasing the power of taxon sampling (Heath et al., 2014), such as 406 Tutusius and Umzantsia from South Africa (Gess and Ahlberg, 2018). However, the current lack 407 of cladistic coding for these taxa excludes them from phylogeny-based analyses. The taxonomic 408 resolution of globally-occurring species, like *Eusthenodon* and *Spodichthys*, also impacts current 409 models of species dispersal history because of their relatively uniform distribution (Long et al., 410 2018). Eusthenodon and Spodichthys represent possible cases where taxonomic resolution is too 411 coarse for phylogeographic analyses. Including these species inhibited our MCMC algorithms 412 from reaching convergence. Widely distributed cosmopolitan species that lack intermediate 413 geographic occurrences increase the uncertainty of parameter estimates within phylogeographic 414 models, as is the case here for these two species.

415 Phylogenetic studies on macroevolution also often fail to incorporate data from the fossil record itself, such as trace fossil occurrences. Non-anatomical data often contribute to our 416 417 understanding of taxonomic originations, including chiridian digit-possessing) (or 418 tetrapodomorphs for which trace fossil evidence exists about 10 million years before the first 419 elpistostegalian body fossils (Niedźwiedzki et al., 2010). The inclusion of additional data from 420 trace fossils could radically alter our current models of species dispersal history. Finally, it is 421 important to note that the sampling bias proxies are also constrained by database curation biases. 422 Phylogenetic studies on macroevolutionary trends now regularly leverage public databases, such 423 as the PBDB, which allows larger and broader studies. It is unclear how patchy entries, on 424 taxonomic occurrences and geological formations, for example, interact with other biases inherent 425 in the fossil record. Caution is therefore warranted when these databases are mined, as is the case

18

426 here.

#### 427 **5.** Conclusions

428 Phylogenetic studies on macroevolution have not previously incorporated geographic 429 context, which could influence a wide variety of analyses. We demonstrate here that 430 phylogeographic methods are influenced by geographic sampling variability. We develop a simple 431 sampling bias proxy that incorporates geographic information and show that it explains variation 432 in estimated dispersal rates. The majority of elevated dispersal rates are associated with large-scale 433 movements between major landmasses that have very few, if any, relevant geological formations 434 in between. Our analysis is also unlikely to be influenced by "Pull of the Recent"-like effects. 435 Although not the first supertree for early tetrapodomorphs (Ruta et al., 2003), this study presents the 436 first (to our knowledge) with branch lengths, making it useable for phylogenetic comparative 437 analyses. The new supertree comprises many of the major clades previously inferred, but also recovers new ones that will be subject to scrutiny in future studies (discussed further in the 438 439 Supplementary Material). This supertree should be useful to researchers who aim to use 440 phylogenetic comparative methods to test hypotheses on the evolution of early tetrapodomorphs. 441 In sum, our study estimates ancestral geographical reconstructions consistent with previously 442 hypothesized dispersal patterns in early tetrapodomorphs. We also find that rates of dispersal are 443 strongly influenced by geographic sampling bias. We suggest that researchers incorporate this 444 proxy in phylogeny-based macroevolutionary studies that could be influenced by spatial 445 distribution of the fossil record.

446

#### 447 Acknowledgements

448 We thank the MSU Macroevolution Lab, Jack Wilson, and Matt Lavin for helpful discussions, as

449	well as David Marjanović and John Long for their helpful reviews. We also thank Nathalie Bardet,
450	Eric Buffetaut, Annelise Folie, Emmanuel Gheerbrant, Alexandra Houssaye, and Michel Laurin
451	for the invitation to contribute to this special issue celebrating the life and accomplishments of
452	Jean-Claude Rage.
453	
454	Funding
455	This research did not receive any specific grant from funding agencies in the public, commercial,
456	or not-for-profit sectors.
457	
458	References
459	Ahlberg, P.E., 1998. Postcranial stem tetrapod remains from the Devonian of Scat Craig,
460	Morayshire, Scotland. Zool. J. Linn. Soc. 122, 99–141.
461	https://doi.org/10.1006/zjls.1997.0115
462	Alroy, J., Marshall, C.R., Bambach, R.K., Bezusko, K., Foote, M., Fürsich, F.T., Hansen, T.A.,
463	Holland, S.M., Ivany, L.C., Jablonski, D., Jacobs, D.K., Jones, D.C., Kosnik, M.A.,
464	Lidgard, S., Low, S., Miller, A.I., Novack-Gottshall, P.M., Olszewski, T.D., Patzkowsky,
465	M.E., Raup, D.M., Roy, K., Sepkoski, J.J., Sommers, M.G., Wagner, P.J., Webber, A., 2001.
466	Effects of sampling standardization on estimates of Phanerozoic marine diversification.
467	PNAS 98, 6261-6266. https://doi.org/10.1073/pnas.111144698
468	Benson, R.B.J., Butler, R.J., 2011. Uncovering the diversification history of marine tetrapods:
469	ecology influences the effect of geological sampling biases. Geological Society, London,
470	Special Publications 358, 191–208. https://doi.org/10.1144/SP358.13
471	Benson, R.B.J., Butler, R.J., Lindgren, J., Smith, A.S., 2010. Mesozoic marine tetrapod diversity:

472	mass extinctions and temporal heterogeneity in geological megabiases affecting vertebrates.
473	Proceedings of the Royal Society B: Biological Sciences 277, 829-834.
474	https://doi.org/10.1098/rspb.2009.1845
475	Benson, R.B.J., Upchurch, P., 2013. Diversity trends in the establishment of terrestrial vertebrate
476	ecosystems: Interactions between spatial and temporal sampling biases. Geology 41, 43-
477	46. https://doi.org/10.1130/G33543.1
478	Benton, M.J., Donoghue, P.C.J., Asher, R.J., Friedman, M., Near, T.J., Vinther, J., 2015.
479	Constraints on the timescale of animal evolutionary history. Palaeontol. Electron. 18, 1-
480	106. https://doi.org/10.26879/424
481	Benton, M.J., Ruta, M., Dunhill, A.M., Sakamoto, M., 2013. The first half of tetrapod evolution,
482	sampling proxies, and fossil record quality. Palaeogeography, Palaeoclimatology,
483	Palaeoecology 372, 18-41. https://doi.org/10.1016/j.palaeo.2012.09.005
484	Budd, G.E., Mann, R.P., 2018. History is written by the victors: The effect of the push of the past
485	on the fossil record. Evolution 72, 2276–2291. https://doi.org/10.1111/evo.13593
486	Clack, J.A., Bennett, C.E., Carpenter, D.K., Davies, S.J., Fraser, N.C., Kearsey, T.I., Marshall,
487	J.E.A., Millward, D., Otoo, B.K.A., Reeves, E.J., Ross, A.J., Ruta, M., Smithson, K.Z.,
488	Smithson, T.R., Walsh, S.A., 2017. Phylogenetic and environmental context of a
489	Tournaisian tetrapod fauna. Nat. Ecol. Evol. 1, 0002. https://doi.org/10.1038/s41559-016-
490	0002
491	Coates, M.I., Friedman, M., 2010. Litoptychus bryanti and characteristics of stem tetrapod
492	neurocrania, in: Elliot, D.K., Maisey, J.G., Yu, X., Miao, D. (Eds.), Morphology, Phylogeny
493	and Paleobiogeography of Fossil Fishes. Verlag Dr. Friedrich Pfeil, München, Germany,
494	pp. 389–416.

- 495 Cope, E.D., 1868. Synopsis of the Extinct Batrachia of North America. Proceedings of the
  496 Academy of Natural Sciences of Philadelphia. 20, 208–221.
- 497 Criscuolo, A., Berry, V., Douzery, E.J.P., Gascuel, O., 2006. SDM: A fast distance-based approach
- 498 for (super)tree building in phylogenomics. Syst. Biol. 55, 740–755.
   499 https://doi.org/10.1080/10635150600969872
- 500 Criscuolo, A., Gascuel, O., 2008. Fast NJ-like algorithms to deal with incomplete distance matrices.
   501 BMC Bioinformatics 9, 166. https://doi.org/10.1186/1471-2105-9-166
- Didier, G., Fau, M., Laurin, M., 2017. Likelihood of tree topologies with fossils and diversification
   rate estimation. Syst. Biol. 66, 964–987. https://doi.org/10.1093/sysbio/syx045
- 504 Didier, G., Laurin, M., 2018. Exact distribution of divergence times from fossil ages and topologies.
   505 bioRxiv 490003. https://doi.org/10.1101/490003
- 506 Didier, G., Royer-Carenzi, M., Laurin, M., 2012. The reconstructed evolutionary process with the 507 fossil record. J. Theor. Biol. 315, 26–37. https://doi.org/10.1016/j.jtbi.2012.08.046
- Dunhill, A.M., Benton, M.J., Newell, A.J., Twitchett, R.J., 2013. Completeness of the fossil record
  and the validity of sampling proxies: a case study from the Triassic of England and Wales.
  Journal of the Geological Society 170, 291–300. https://doi.org/10.1144/jgs2012-025
- Dunhill, A.M., Benton, M.J., Twitchett, R.J., Newell, A.J., 2014a. Testing the fossil record:
  Sampling proxies and scaling in the British Triassic–Jurassic. Palaeogeography,
  Palaeoclimatology, Palaeoecology 404, 1–11. https://doi.org/10.1016/j.palaeo.2014.03.026
- Dunhill, A.M., Hannisdal, B., Benton, M.J., 2014b. Disentangling rock record bias and commoncause from redundancy in the British fossil record. Nature Communications 5, 4818.
  https://doi.org/10.1038/ncomms5818
- 517 Foote, M., 2003. Origination and Extinction through the Phanerozoic: A New Approach. The

518	Journal of Geology 111, 125-148. https://doi.org/10.1086/345841
519	Friedman, M., Coates, M.I., Anderson, P., 2007. First discovery of a primitive coelacanth fin fills
520	a major gap in the evolution of lobed fins and limbs. Evol. Dev. 9, 329-337.
521	https://doi.org/10.1111/j.1525-142X.2007.00169.x
522	Gascuel, O., 1997. Concerning the NJ algorithm and its unweighted version, UNJ, in: Roberts, F.,
523	Rzhetsky, A. (Eds.), Mathematical Hierarchies and Biology. American Mathematical Soc.,
524	Providence, RI, pp. 149–170.
525	Gauthier, J., Cannatella, D., de Queiroz, K., Kluge, A.G., Rowe, T., 1989. Tetrapod phylogeny, in:
526	Fernholm, B., Bremer, K., Jörnvall, H. (Eds.), The Hierarchy of Life. Elsevier Science
527	Publishers B. V. (Biomedical Division), Amsterdam, Netherlands.
528	Gavryushkina, A., Welch, D., Stadler, T., Drummond, A.J., 2014. Bayesian Inference of Sampled
529	Ancestor Trees for Epidemiology and Fossil Calibration. PLOS Comput Biol 10, e1003919
530	https://doi.org/10.1371/journal.pcbi.1003919
531	Gess, R., Ahlberg, P.E., 2018. A tetrapod fauna from within the Devonian Antarctic Circle. Science
532	360, 1120–1124. https://doi.org/10.1126/science.aaq1645
533	Heath, T.A., Huelsenbeck, J.P., Stadler, T., 2014. The fossilized birth-death process for coherent
534	calibration of divergence-time estimates. PNAS 111, E2957–E2966.
535	https://doi.org/10.1073/pnas.1319091111
536	Jablonski, D., Roy, K., Valentine, J.W., Price, R.M., Anderson, P.S., 2003. The Impact of the Pull
537	of the Recent on the History of Marine Diversity. Science 300, 1133-1135.
538	https://doi.org/10.1126/science.1083246
539	Koch, C.F., 1978. Bias in the Published Fossil Record. Paleobiology 4, 367–372.
540	Lakner, C., van der Mark, P., Huelsenbeck, J.P., Larget, B., Ronquist, F., 2008. Efficiency of

- Markov chain Monte Carlo tree proposals in Bayesian phylogenetics. Syst. Biol. 57, 86–
  103. https://doi.org/10.1080/10635150801886156
- Laurin, M., 1998. The importance of global parsimony and historical bias in understanding
   tetrapod evolution. Part I. Systematics, middle ear evolution and jaw suspension. Ann. Sci.
- 545 Nat. Zoo. 19, 1–42. https://doi.org/10.1016/S0003-4339(98)80132-9
- Lloyd, G.T., 2012. A refined modelling approach to assess the influence of sampling on
  palaeobiodiversity curves: new support for declining Cretaceous dinosaur richness. Biol.
  Lett. 8, 123–126. https://doi.org/10.1098/rsbl.2011.0210
- Long, J.A., Clement, A.M., Choo, B., 2018. New insights into the origins and radiation of the mid Palaeozoic Gondwanan stem tetrapods. Earth and Environmental Science Transactions of
   The Royal Society of Edinburgh 1–17. https://doi.org/10.1017/S1755691018000750
- Marjanović, D., Laurin, M., 2019. Phylogeny of Paleozoic limbed vertebrates reassessed through
   revision and expansion of the largest published relevant data matrix. PeerJ 6, e5565.
   https://doi.org/10.7717/peerj.5565
- 555 Marshall, J.E.A., Reeves, E.J., Bennett, C.E., Davies, S.J., Kearsey, T.I., Millward, D., Smithson,
- T.R., Browne, M.A.E., 2019. Reinterpreting the age of the uppermost "Old Red Sandstone"
  and Early Carboniferous in Scotland. Earth Env. Sci. T. R. So. 109, 265–278.
  https://doi.org/10.1017/S1755691018000968
- Niedźwiedzki, G., Szrek, P., Narkiewicz, K., Narkiewicz, M., Ahlberg, P.E., 2010. Tetrapod
  trackways from the early Middle Devonian period of Poland. Nature 463, 43–48.
  https://doi.org/10.1038/nature08623
- 562 O'Donovan, C., Meade, A., Venditti, C., 2018. Dinosaurs reveal the geographical signature of an
  563 evolutionary radiation. Nature Ecology & Evolution 2, 452.

### 564 https://doi.org/10.1038/s41559-017-0454-6

- Pardo, J.D., Szostakiwskyj, M., Ahlberg, P.E., Anderson, J.S., 2017. Hidden morphological
  diversity among early tetrapods. Nature 546, 642–645.
  https://doi.org/10.1038/nature22966
- R Core Team, 2018. R: A Language and Environment for Statistical Computing. R Foundation for
   Statistical Computing, Vienna, Austria.
- Rambaut, A., Drummond, A.J., Xie, D., Baele, G., Suchard, M.A., 2018. Posterior Summarization
  in Bayesian Phylogenetics Using Tracer 1.7. Syst Biol 67, 901–904.
- 572 https://doi.org/10.1093/sysbio/syy032
- 573 Raup, D.M., Boyajian, G.E., 1988. Patterns of Generic Extinction in the Fossil Record.
  574 Paleobiology 14, 109–125.
- 575 Revell, L.J., 2012. phytools: an R package for phylogenetic comparative biology (and other things).
- 576 Methods in Ecology and Evolution 3, 217–223. https://doi.org/10.1111/j.2041-577 210X.2011.00169.x
- 578 Robinson, D.F., Foulds, L.R., 1981. Comparison of phylogenetic trees. Math. Biosci. 53, 131–147.
   579 https://doi.org/10.1016/0025-5564(81)90043-2
- Ronquist, Fredrik, Klopfstein, S., Vilhelmsen, L., Schulmeister, S., Murray, D.L., Rasnitsyn, A.P.,
  2012. A total-evidence approach to dating with fossils, applied to the early radiation of the
  Hymenoptera. Syst. Biol. 61, 973–999. https://doi.org/10.1093/sysbio/sys058
- 583 Ronquist, F., Teslenko, M., van der Mark, P., Ayres, D., Darling, A., Höhna, S., Larget, B., Liu, L.,
- 584 Suchard, M.A., Huelsenbeck, J.P., 2012. MrBayes 3.2: Efficient Bayesian phylogenetic
- 585 inference and model choice across a large model space. Systematic Biology.
- 586 Rothkugel, S., Varela, S., 2015. paleoMap: An R-package for getting and using paleontological

Sakamoto, M., Benton, M.J., Venditti, C., 2016a. Dinosaurs in decline tens of millions of years

25

587 maps.

588

589	before their final extinction. PNAS 113, 5036–5040.
590	https://doi.org/10.1073/pnas.1521478113
591	Sakamoto, M., Venditti, C., Benton, M.J., 2016b. 'Residual diversity estimates' do not correct for
J)1	Sakamoto, W., Venditti, C., Benton, W.J., 20100. Residual diversity estimates do not correct for
592	sampling bias in palaeodiversity data. Methods Ecol Evol n/a-n/a.
593	https://doi.org/10.1111/2041-210X.12666
594	Schliep, K.P., 2011. phangorn: Phylogenetic analysis in R. Bioinformatics 27, 592-593.
595	https://doi.org/10.1093/bioinformatics/btq706
596	Signor, P.W., Lipps, J.H., 1982. Sampling bias, gradual extinction patterns, and catastrophes in the
597	fossil record. Geological Society of America Special Publication 190, 291–296.
598	Stadler, T., 2010. Sampling-through-time in birth-death trees. J. Theor. Biol. 267, 396-404.
599	https://doi.org/10.1016/j.jtbi.2010.09.010
600	Swartz, B., 2012. A marine stem-tetrapod from the Devonian of Western North America. PLoS
601	ONE 7, e33683. https://doi.org/10.1371/journal.pone.0033683
602	Tennant, J.P., Mannion, P.D., Upchurch, P., 2016a. Environmental drivers of crocodyliform
603	extinction across the Jurassic/Cretaceous transition. Proc. R. Soc. B 283, 20152840.
604	https://doi.org/10.1098/rspb.2015.2840
605	Tennant, J.P., Mannion, P.D., Upchurch, P., 2016b. Sea level regulated tetrapod diversity dynamics
606	through the Jurassic/Cretaceous interval. Nature Communications 7, 12737.
607	https://doi.org/10.1038/ncomms12737
608	Venditti, C., Meade, A., Pagel, M., 2011. Multiple routes to mammalian diversity. Nature 479,

609 393–396. https://doi.org/10.1038/nature10516

26

610	Xie, W., Lewis, P.O., Fan, Y., Kuo	, L., Chen,	МН.,	2011. Impro	oving	Margina	al Likelih	ood
611	Estimation for Bayesian P	hylogenetic	Model	Selection.	Syst	Biol 6	50, 150–1	60.
612	https://doi.org/10.1093/sysbic	syq085/						

- Zhang, C., Stadler, T., Klopfstein, S., Heath, T.A., Ronquist, F., 2016. Total-Evidence Dating under
   the Fossilized Birth–Death Process. Syst Biol 65, 228–249.
   https://doi.org/10.1093/sysbio/syv080
- Zhu, M., Ahlberg, P.E., Zhao, W.-J., Jia, L.-T., 2017. A Devonian tetrapod-like fish reveals
  substantial parallelism in stem tetrapod evolution. Nat. Ecol. Evol. 1, 1470–1476.
  https://doi.org/10.1038/s41559-017-0293-5
- 619

#### 620 Figure Captions

621 1. Example of how the regional-level formation count proxy is calculated. A) Five major geographic regions are highlighted by color in the Devonian map. Red arrows represent a branch-622 specific dispersal path to species A, beginning in Southern Euramerica and ending in Eastern 623 624 Gondwana. The blue arrow represents the dispersal path to species B. B) The phylogeny of species 625 A and B scaled by time, with equal branch lengths to both species, and colored to represent the 626 rate of dispersal (red is fast, blue is slow). For every branch of the tree, the number of formations 627 is counted for every region and for each geological age covered by the dispersal pathway. It is then weighted by the number of geological ages and geographic regions covered. Under the Western 628 629 Gondwana route scenario, the branch to species A covers three geographic regions, while the branch to species B only covers one. Assuming both branches cover only one geological age, the 630 631 high dispersal rate for species A can be explained by the lack of recorded geological formations in 632 Western Gondwana. C) A line plot of the formation counts through time, colored by geographic region according to the Devonian map above, shows temporal and geographic variability.

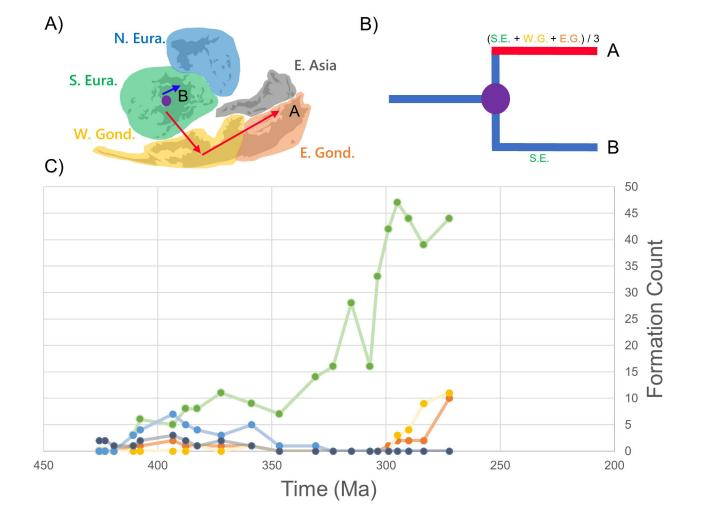
634

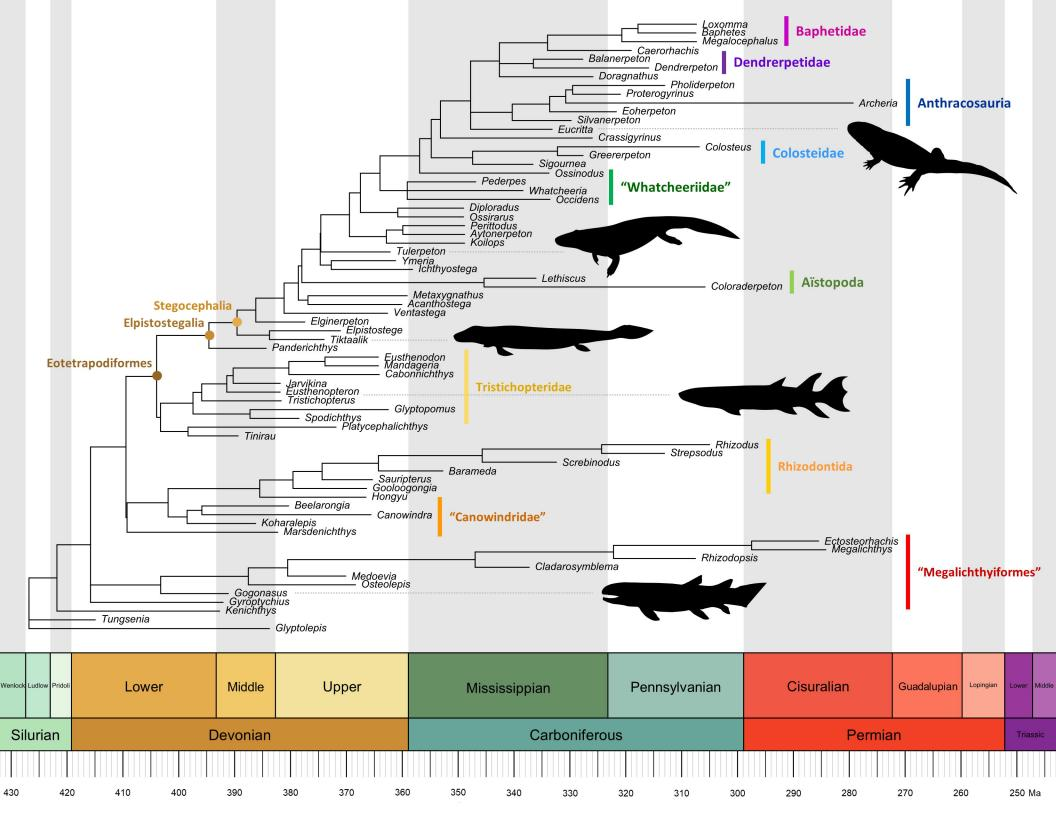
2. The time-scaled tetrapodomorph supertree. Taxonomic groups in quotes are not monophyletic.
Here, *Glyptolepis*, a dipnomorph, is the outgroup. We downloaded the silhouettes from
phylopic.org: *Eucritta* and *Greererpeton* by Dmitry Bogdanov (vectorized by Michael Keesey), *Eusthenopteron* by Steve Coombs (vectorized by Michael Keesey), and *Gogonasus* and *Tiktaalik*by Nobu Tamura (CC BY-SA 3.0).

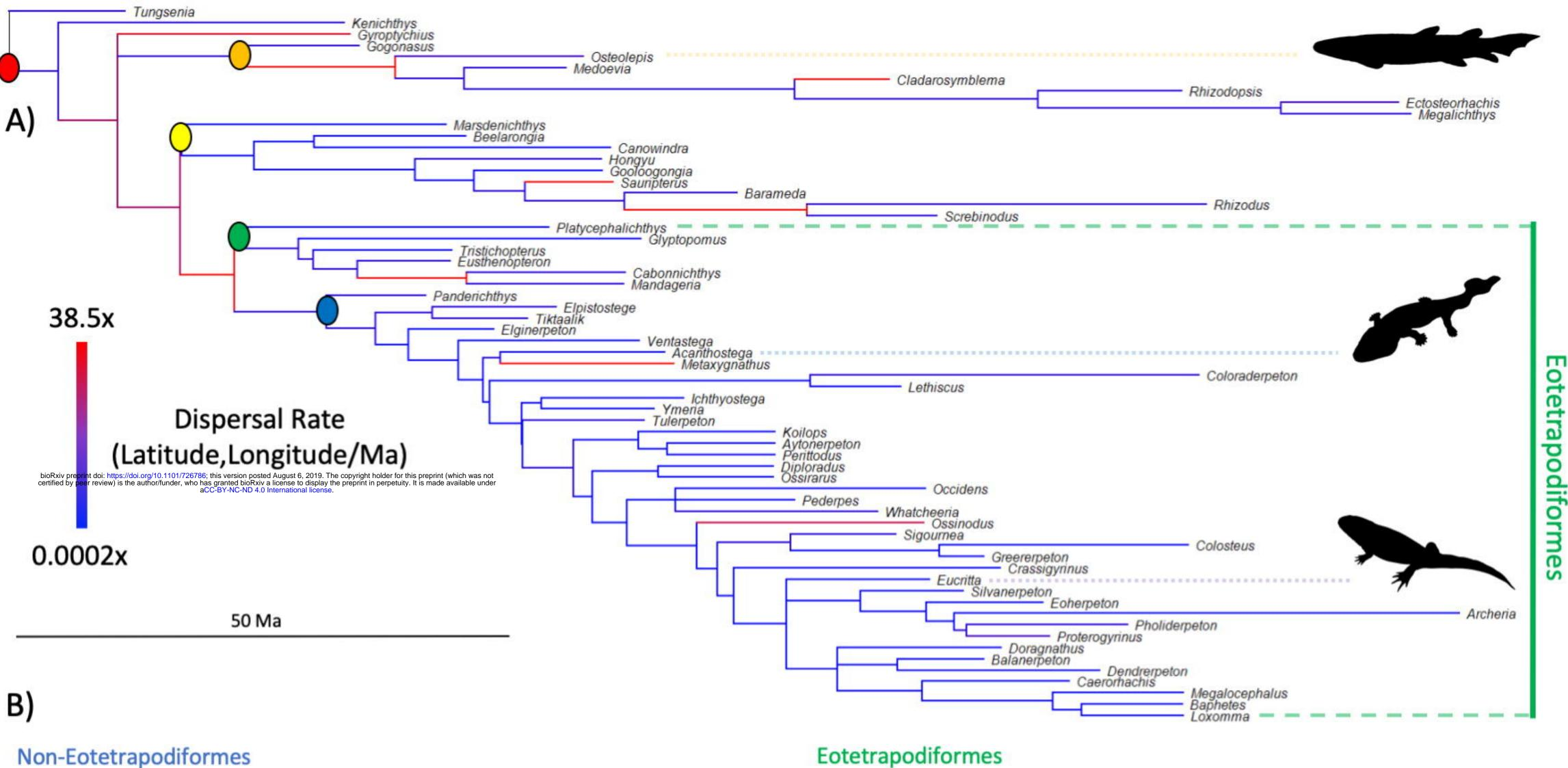
640

641 3. A) Trimmed tetrapodomorph phylogeny with mapped rates of dispersal. Cooler (bluish) colors 642 represent slower rates and warmer (reddish) colors represent faster rates. B) Non-eotetrapodiform 643 (left in blue) and eotetrapodiform (right in green) trees and taxon paleolocations plotted on a map 644 of the Middle Devonian. Transparent polygons illustrate broad geographic regions of sampled taxa in Southern Euramerica, Eastern Gondwana, and East Asia. Numbers show the total number of 645 646 geological formations recorded from each major geographic region (Eastern Gondwana and East 647 Asia combined). Colored circles show average paleolocations of major clades estimated by the 'geo' model and indicated in the tree above. Red circle: Tetrapodomorpha, orange: 648 649 "Megalichthyiformes", yellow: "Canowindridae" + Rhizodontidae, green: Tristichopteridae, and 650 blue: Elpistostegalia. Phylogeny with mapped dispersal rates was produced in BayesTrees 651 (http://www.evolution.rdg.ac.uk/BayesTrees.html). Middle Devonian tree and paleolocation plots 652 were made using the 'phylo-to-map' function in the R package, phytools (Revell, 2012). Middle 653 Devonian map was sourced from the R package, paleoMap (Rothkugel and Varela, 2015). 654 Tetrapodomorph silhouettes were sourced from phylopic.org: Eucritta by Dmitry Bogdanov 655 (vectorized by T. Michael Keesey), Osteolepis by Nobu Tamura, and Acanthostega by Mateus Zica.

657	4. A) Scatter-plot of the average dispersal rates over the regional-level formation counts for each
658	branch of the phylogeny, using the Northern Euramerica + East Asia route scenario. Points colored
659	by the dispersal rate being above (red) or below (blue) two standard deviations greater than the
660	average rate across the tree. B) Histogram of the bootstrapped U-statistics. Values outside of the
661	95% confidence interval are grayed out. The median and null expected U-statistics are indicated
662	by the red and blue dotted lines, respectively. The null expected U-statistic is based on the null
663	hypothesis that 50% of the branches with low dispersal rates will have a greater regional-level
664	formation count than branches with higher rates. Rejecting the null hypothesis suggests that
665	estimated dispersal rates are biased and correlate with regional-level formation count.







# Non-Eotetrapodiformes

